Metal Quinolinolate−Fullerene(s) Donor−Acceptor Complexes: Evidence for Organic LED Molecules Acting as Electron Donors in Photoinduced Electron-Transfer Reactions

Francis D'Souza,*,[†] Eranda Maligaspe,[†] Melvin E. Zandler,[†]
Navaneetha K. Subbaiyan,[†] Kei Ohkubo,[‡] and Shunichi Fukuzumi*,[‡]

Department of Chemistry, Wichita State University, 1845 Fairmount, Wichita, Kansas 67260-0051, and Department of Material and Life Science, Graduate School of Engineering, Osaka University, SORST, Japan Science and Technology Agency, Suita, Osaka, 565-0871, Japan

Received July 1, 2008; E-mail: fukuzumi@chem.eng.osaka-u.ac.jp; Francis.DSouza@wichita.edu

Abstract: Tris(quinolinolate)aluminum(III) (AlQ_3) is the most widely used molecule in organic light-emitting devices. There exists a strong demand for understanding the photochemical and photophysical events originating from this class of molecules. This paper provides the first report on the electron donor ability of MQ_n (M = Al or Zn for n = 3 or 2) complexes covalently connected to a well-known electron acceptor, fullerene. To accomplish this, fullerene was functionalized with 8-hydroxyquinoline at different ligand positions and their corresponding zinc(II) and aluminum(III) complexes were formed in situ. The weakly fluorescent metal quinolinolate−fullerene complexes formed a new class of donor−acceptor conjugates. The stoichiometry and structure of the newly formed metal quinolinolate−fullerene complexes were established from various spectroscopic methods including matrix-assisted laser desorption/ionization time-of-flight mass spectrometry and computational density functional theory studies. Electrochemical studies involving free-energy calculations suggested the possibility of photoinduced electron transfer from excited metal−quinolinolate complex to the appended fullerene entity. Femtosecond transient absorption studies confirmed such a claim and analysis of the kinetic data allowed us to establish the different photophysical events in sufficient detail. The novel features of this class of donor−acceptor conjugates include faster charge recombination compared to charge separation and decay of the charge-separated state to populate the low-lying fullerene triplet state in competition with direct charge recombination to the ground state.

Introduction

The tris(quinolinolate)aluminum complex (AlQ_3) has become the most important material for developing electron-transport and light emitting small molecule-based organic light-emitting diodes (OLED), from the time it was first reported in 1987 by Tang and Vanslyke.[1] Since then, the charge-transporting characteristics and luminescent properties of many MQ_3 and MQ_2 derivatives (M = metal) having different substituents on the quinolinolate ring have been reported.[2,3] To improve the

OLED performance, control over the dynamics and migration of excited states are recognized to be critical factors, consequently, widespread attention is devoted for this research topic.[4]

For maximum OLED light output,[5] harvesting the triplet excited states produced during electron−hole recombination[6] is an essential step. Often, this is achieved by (i) dispersing a phosphorescent dopant energy acceptor (A) molecule in the host

[†] Wichita State University.
[‡] Osaka University, SORST.

(1) Tang, C. W.; Vanslyke, S. A. *Appl. Phys. Lett.* **1987**, *51*, 913.
(2) (a) Burrows, P. E.; Sapochak, L. S.; McCarty, D. M.; Forrest, S. R.; Thompson, M. E. *Appl. Phys. Lett.* **1994**, *64*, 2718. (b) Kido, J.; Iizumi, Y. *Chem. Lett.* **1997**, 963. (c) Burrows, P. E.; Shen, Z.; Bulovic, V.; McCarty, D. M.; Forrest, S. R.; Cronin, J. A.; Thompson, M. E. *J. Appl. Phys.* **1996**, *79*, 7991. (d) Matsumura, M.; Akai, T. *Jpn. J. Appl. Phys., Part 1* **1996**, *35*, 5357. (e) Chen, C. H.; Shi, J. M. *Coord. Chem. Rev.* **1998**, *171*, 161. (f) Pohl, R.; Anzenbacher, P., Jr *Org. Lett.* **2003**, *5*, 2769–2772. (g) Anderson, J. D.; McDonald, E. M.; Lee, P. A.; Anderson, M. L.; Ritchie, E. L.; Hall, H. K.; Hopkins, T.; Mash, E. A.; Wang, J.; Padias, A.; Thayumanavan, S.; Barlow, S.; Marder, S. R.; Jabbour, G. E.; Shaheen, S.; Kippelen, B.; Peyghambarian, N.; Wightman, R. M.; Armstrong, N. R. *J. Am. Chem. Soc.* **1988**, *120*, 9646–9655. (h) La Deda, M.; Grisolia, A.; Aiello, I.; Crispini, A.; Ghedini, M.; Belviso, S.; Amati, M.; Lelj, F. *Dalton Trans.* **2004**, 2424–2431. (i) Wang, J.; Oyler, K. D.; Bernhard, S. *Inorg. Chem.* **2007**, *46*, 5700–5706. (j) Bei, X.; Swewnson, D. C.; Jordan, R. F. *Organometallics* **1997**, *16*, 3282–3302.

(3) For electroluminescence applications of bis(8-hydroxyquinoline) zinc complexes see: (a) Hamada, Y.; Sano, T.; Fujita, N.; Fujii, T.; Nishio, Y.; Shibata, K. *Jpn. J. Appl. Phys.* **1993**, *32*, L514. (b) Donze, N.; Pechy, P.; Grätzel, M.; Schaer, M.; Zuppioli, L. *Chem. Phys. Lett.* **1999**, *315*, 405. (c) Thomsen, D. L.; Phely-Bobin, T.; Papadimitrakopoulos, F. *J. Am. Chem. Soc.* **1998**, *120*, 6177. (d) Sapochak, L. S.; Benincasa, F. E.; Schofield, R. S.; Baker, J. L.; Riccio, K. K. C.; Fogarty, D.; Kohlmann, H.; Ferris, K. F.; Burrows, P. E. *J. Am. Chem. Soc.* **2002**, *124*, 6119–6125.
(4) (a) *Organic Light-Emitting Materials and Devices*; Li, Z., Meng, H., Eds.; CRC: Boca Raton, FL, 2007. (b) *Organic Electroluminescence*; Kafafi, Z. H., Ed.; CRC Press: Boca Raton, FL, 2005.
(5) (a) Baldo, M. A.; Forrest, S. R. *Phys. Rev. B* **2000**, *62*, 10958. (b) Adachi, C.; Kwong, R. C.; Djurovich, P.; Adamovich, V.; Baldo, M. A.; Thompson, M. E.; Forrest, S. R. *Appl. Phys. Lett.* **2001**, *79*, 2082.
(6) (a) Koehler, A.; Wilson, J. *Org. Electron.* **2003**, *4*, 179. (b) Baldo, M. A.; O'Brien, D. F.; You, Y.; Shoustikov, A.; Sibley, S.; Thompson, M E.; Forrest, S. R. *Nature* **1998**, *395*, 151. (c) Wilson, J. S.; Dhoot, A. S.; Seeley, A. J. A. B.; Khan, M. S.; Koehler, A.; Friend, R. H. *Nature* **2001**, *413*, 828.

energy donor (D) matrix,[7] or (ii) covalently linking the energy donor and energy acceptor entities with suitable spacers.[8] Although the former approach is easy to perform, incipient phase separation and uneven distribution of the donor−acceptor (D−A) distances results in diminished light output from the device.[7] From this viewpoint, the latter approach seems to be suitable where alignment of energy levels of the entities and the nature of the spacer for maximum excitation transfer,[9] resulting in improved OLED efficiency, can be accomplished.[8] However, the dynamics of triplet-energy transfer is often excluded by low efficiency of the intersystem crossing (ISC) compared to competing fluorescence, nonradiative decay, and singlet energy transfer processes.[10] Thus, improving our understanding on the photochemical and photophysical events in detail is required for designing highly competent donor−acceptor type OLED materials.

A literature survey shows that there are a large number of examples of AlQ_3 involved in photoinduced energy transfer related to OLED applications;[2,3,7,8] however, the ability of this photosensitizer complex acting as an electron donor has never been tested.[11] In our continued quest for finding electron donors for variety of electron-transfer applications,[12−16] in the present study we have designed novel electron donor−acceptor complexes involving aluminum and zinc quinolinolate complexes as electron donors. For the choice of electron acceptor, we have

Chart 1

M = Al(III) n = 3; Al**1**₃
M = Zn(II) n = 2; Zn**1**₂

M = Al(III) n = 3; Al**2**₃
M = Zn(II) n = 2; Zn**2**₂
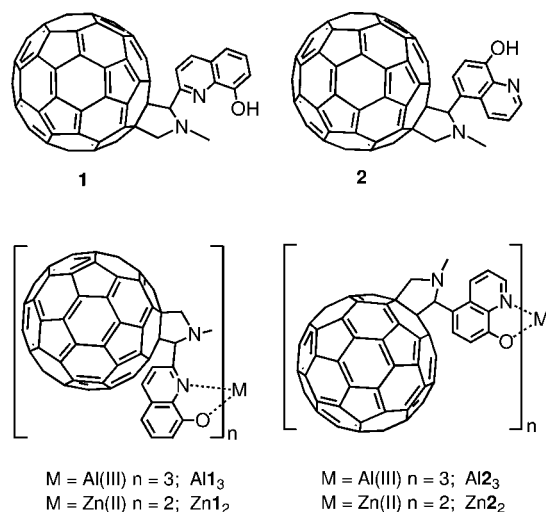
employed fullerene,[17] C_{60} because of its outstanding electron acceptor properties which include ability to reversibly undergo up to six one-electron reductions,[18] diagnostic radical anion signal in the near-IR region to provide evidence of electron transfer quenching mechanism,[15,16] requiring low reorganization energy in electron transfer reactions;[19] and weak phosphorescence emission.[20] The calculated energetics of the charge-separated state of these dyads, $MQ_n^{\bullet+}-C_{60}^{\bullet-}$ (M = Al and Zn for n = 3 and 2), suggests it to be high energy state. Consequently, the decay of this state would result in populating the low-lying triplet energy level of the acceptor, in addition to the competitive charge recombination to the ground state. This hypothesis has also been verified in the present study.

For the design, two 8-hydroxyquinoline appended fullerenes, namely, 2-(1-methylfulleropyrrolidin-2-yl)-quinolin-8-ol **1** and 5-(1-methylfulleropyrrolidin-2-yl)-quinolin-8-ol **2**, were synthesized. As demonstrated here, both fullerene derivatives **1** and **2** bind aluminum(III) and zinc(II) and form supramolecular complexes of 1:3 and 1:2 metal/ligand stoichiometry (see Chart 1 for structures). As predicted, the MQ_n parts of the supramolecular complexes are luminescent, however, with much diminished emission intensity compared to their pristine MQ_n complexes. Detailed photochemical investigations involving femtosecond transient absorption technique demonstrated that the quenching is indeed due to electron transfer from the singlet excited MQ_n to the appended fullerene entity generating high energy charge-separated states. In addition, we are able to show that the charge-separated state decays to populate the low-lying triplet excited-state of fullerene, in addition to competitively

(7) (a) Sandee, A. J.; Williams, C. K.; Evans, N. R.; Davies, J. E.; Boothby, C. E.; Koehler, A.; Friend, R. H.; Holmes, A. B. *J. Am. Chem. Soc.* **2004**, *126*, 7041. (b) Jarikov, V. V.; Kondakov, D. Y.; Brown, C. T. *J. Appl. Phys.* **2007**, *102*, 1–6. (c) Shi, Y. M.; Deng, Z.-B.; Xu, D.-H.; Chen, Z.; Li, X.-F. *Displays* **2007**, *28*, 97–100. (d) Huang, J.-Z.; Xu, Z.; Zhao, S.-L.; Zhang, F.-J.; Wang, Y. *Appl. Surf. Sci.* **2007**, *253*, 4542–4545. (e) Zhilin, Z.; Xueyin, J.; Shaohong, X. *Thin Solid Films* **2000**, *363*, 61–63.

(8) (a) Montes, V. A.; Pèrez-Bolìvar, C.; Agarwal, N.; Shinar Anzenbacher, J., Jr *J. Am. Chem. Soc.* **2006**, *128*, 12436. (b) Montes, V.A.; Pèrez-Bolìvar, C.; Estrada, L. A.; Shinar, J.; Anzenbacher, P, Jr. *J. Am. Chem. Soc.* **2007**, *129*, 12598–12599. (c) Montes, V. A.; Anzenbache, P., Jr *PMSE Preprints* **2007**, *96*, 755–756. (d) Tsutsumi, N.; Masaki, Y. J. *Opt. Soc. Am., B.* **2006**, *23*, 842–845. (e) Hamada, Y.; Kanno, H.; Tsujioka, T.; Takahashi, H.; Usuki, T. *Appl. Phys. Lett.* **1999**, *75*, 1682–1684.

(9) Welter, S.; Lafolet, F.; Cecchetto, E.; Vergeer, F.; De Cola, L. *ChemPhysChem* **2005**, *6*, 2417.

(10) Hayes, R. T.; Walsh, C. J.; Wasielewski, M. R. *J. Phys. Chem., A* **2004**, *108*, 3253.

(11) For photoinduced electron transfer from the metal substrates to AlQ_3, see: (a) Ino, D.; Watanabe, K.; Takagi, N.; Matsumoto, Y. *Phys. Rev. B* **2005**, *71*, 115427.

(12) (a) Gust, D.; Moore, T. A. In *The Porphyrin Handbook*; Kadish, K. M., Smith, K. M., Guilard, R., Eds.; Academic Press: Burlington, MA, 2000; Vol. 8, pp 153−190. (b) Gust, D.; Moore, T. A.; Moore, A. L. In *Electron Transfer in Chemistry*; Balzani, V., Ed.; Wiley-VCH: Weinheim, Germany, 2001; Vol. 3, pp 272−336.

(13) (a) Prato, M. *J. Mater. Chem.* **1997**, *7*, 1097–1109. (b) Martín, N.; Sánchez, L.; Illescas, B.; Pérez, I. *Chem. Rev.* **1998**, *98*, 2527–2547. (c) Diederich, F.; Gómez-López, M. *Chem. Soc. Rev.* **1999**, *28*, 263–277.

(14) Wasielewski, M. R. *Chem. Rev.* **1992**, *92*, 435.

(15) (a) Fukuzumi, S.; Guldi, D. M. In *Electron Transfer in Chemistry*; Balzani, V., Ed.; Wiley-VCH: Weinheim, Germany, 2001; Vol. 2, pp 270−337. (b) Guldi, D. M. *Chem. Commun.* **2000**, 321–327. (c) Guldi, D. M.; Prato, M. *Acc. Chem. Res.* **2000**, *33*, 695–703. (d) Guldi, D. M. *Chem. Soc. Rev.* **2002**, *31*, 22–36. (e) Meijer, M. E.; van Klink, G. P. M.; van Koten, G. *Coord. Chem. Rev.* **2002**, *230*, 141–163.

(16) (a) El-Khouly, M. E.; Ito, O.; Smith, P. M.; D'Souza, F. *J. Photochem. Photobiol. C* **2004**, *5*, 79–104. (b) Imahori, H.; Fukuzumi, S. *Adv. Funct. Mater.* **2004**, *14*, 525–536. (c) D'Souza, F.; Ito, O. *Coord. Chem. Rev.* **2005**, *249*, 1410–1422. (d) Sanchez, L.; Martin, N.; Guldi, D. M. *Angew. Chem., Int. Ed.* **2005**, *44*, 5374–5382. (e) Bouamaied, T. I.; Coskun, E. S. *Struct. Bonding (Berlin)* **2006**, *121*, 1–147. (f) Chitta, R.; D'Souza, F. *J. Mater. Chem.* **2008**, *18*, 1440–1471. (g) Fukuzumi, S.; Kojima, T. *J. Mater. Chem.* **2008**, *18*, 1427–1439. (h) Fukuzumi, S. *Phys. Chem. Chem. Phys.* **2008**, *10*, 2283–2297.

(17) (a) Kroto, H. W.; Heath, J. R.; O'Brien, S. C.; Curl, R. F.; Smalley, R. E. *Nature* **1985**, *318*, 162–163. (b) Kratschmer, W.; Lamb, L. D.; Fostiropoulos, F.; Huffman, D. R. *Nature* **1990**, *347*, 354–358. (c) *Fullerene and Related Structures*; Hirsch, A., Ed.; Springer: Berlin, 1999; Vol. 199.

(18) (a) Allemand, P. M.; Koch, A.; Wudl, F.; Rubin, Y.; Diederich, F.; Alvarez, M. M.; Anz, S. J.; Whetten, R. L. *J. Am. Chem. Soc.* **1991**, *113*, 1050–1051. (b) Xie, Q.; Perez-Cordero, E.; Echegoyen, L. *J. Am. Chem. Soc.* **1992**, *114*, 3978–3980.

(19) (a) Fukuzumi, S.; Nakanishi, I.; Suenobu, T.; Kadish, K. M. *J. Am. Chem. Soc.* **1999**, *121*, 3468–3474. (b) Fukuzumi, S.; Ohkubo, K.; Imahori, H.; Guldi, D. M. *Chem.—Eur. J.* **2003**, *9*, 1585–1593. (c) Imahori, H.; El-Khouly, M. E.; Fujitsuka, M.; Ito, O.; Sakata, Y.; Fukuzumi, S. *J. Phys. Chem. A* **2001**, *105*, 325–332.

(20) (a) Wasielewski, M. R.; O'Neil, M. P.; Lykke, K. R.; Pellin, M. J.; Gruen, D. M. *J. Am. Chem. Soc.* **1991**, *113*, 2776–2777. (b) Orlandi, G.; Fabrizia, N. *Photochem. Photobiol. Sci.* **2002**, *1*, 289–308.

decaying to the ground-state via a charge recombination process. Although the phosphorescence of C_{60} is too weak for any OLED application, the first detailed mechanistic study presented herein on populating the triplet state of the acceptor via a charge-separated intermediate provides an alternate approach for excitation energy transfer of MQ_n.

Experimental Section

Chemicals. Tetra-*n*-butylammonium perchlorate, $(n\text{-Bu})_4NClO_4$ was obtained from Fluka Chemicals. 8-Hydroxyquinoline and 2-formyl-8-hydroxyquinoline were procured from Aldrich Chemicals. All other reagents and solvents were procured from Fisher Chemicals. Benzonitrile used in spectral studies was freshly distilled over P_2O_5 in vacuo to remove the impurity.[21]

The syntheses of 8-hydroxyquinoline appended fullerene derivatives **1** and **2** were accomplished by reacting 2- or 5-formyl-8-hydroxyquinoline with C_{60} and sarcosine using the standard Prato method of fulleropyrrolidine synthesis.[22] The structural integrity of **1** and **2**, and the subsequent metal complexes, were established from UV—vis, ESI-mass, and NMR (^{1}H and ^{13}C) spectroscopic as well as electrochemical methods.

Synthesis. 5-formyl-8-hydroxyquinoline. 8-Hydroxyquinoline (5 g, 34.4 mmol) was dissolved in a solution of aqueous NaOH and ethanol and the reaction mixture was stirred at 40 °C. The pale opalescent mixture was heated and 8 mL of chloroform was added over 40 min. The resulting black mixture was heated at reflux for 12 h. Subsequently, the solvent was evaporated under reduced pressure, and the semisolid mass was poured into 200 mL of cold water and pH was adjusted to 2.0 with conc. HCl. The brown precipitate was filtered off, crushed, and dried. The crude compound was purified by column chromatography (silica gel, ethyl acetate) to give the product (495 mg, 8.3%). ^{1}H NMR (300 MHz, CDCl$_3$): $\delta = 10.14$ (s, 1H), 9.69 (dd, $J = 8.65$ Hz, 1H), 8.87 (dd, $J = 4.26$ Hz, 1H), 8.00 (d, $J = 8.03$, 1H), 7.66 (q, 4.31 Hz, 1H), 7.28 ppm (d, $J = 7.89$ Hz, 1H). UV—vis (PhCN): $\lambda_{max} = 330.0$, 388.2 nm.

2-(1-Methylfulleropyrrolidin-2-yl)-quinolin-8-ol, 1. A solution of C_{60} (100 mg, 0.138 mmol), *N*-methylglycine (24 mg, 0.277 mmol), and 2-formyl-8-hydroxyquinoline (72 mg, 0.416 mmol) in toluene (100 mL) was heated at reflux for 4 h before the solvent was evaporated. The crude product was purified by column chromatography (silica gel, hexane/toluene 5:95) to give the product (29 mg, 22.7%). ^{1}H NMR (300 MHz, CDCl$_3$): $\delta = 8.28$ (d, $J = 8.12$ Hz, 1H), 8.19 (d, $J = 8.24$ Hz, 1H), 7.44 (t, $J = 7.95$, 1H), 7.33 (dd, $J = 8.42$ Hz, 1H), 7.15 (d, $J = 7.59$ Hz, 1H), 5.38 (s, 1H), 5.05 (d, $J = 9.51$ Hz, 1H), 4.38 (d, $J = 9.51$ Hz, 1H), 2.87 ppm (s, 3H); ^{13}C NMR (CDCl$_3$:CS$_2$): 42.83 (N-CH3); 67.01 (N-CH2); 84.56 (N-CH), 110.01, 118.42, 118.44, 130.01, 129.05, 136.77, 137.54, 146.71, 153.01 (hydroxyquinoline ring), 72.58, 75.58, 136.04, 136.85, 137.50, 139.50, 139.85, 139.70, 141.22, 141.27, 141.73, 141.85, 141.90, 141.98, 142.08, 142.10, 142.20, 142.58, 142.62, 143.00, 144.35, 144.49, 144.60, 145.19, 145.25, 145.38, 145.40, 145.44, 145.50, 145.60, 145.63, 145.75, 145.98, 146.01, 146.18, 146.19, 146.20, 146.30, 147.20, 147.28, 150.80, 153.66, 154.80 (fullerene moiety). UV—vis (PhCN): $\lambda_{max} = 325.2$, 431.5, 702.0 nm. Mass (APCI mode in CH$_2$Cl$_2$): calcd, 921.0; found, 921.2.

5-(1-Methylfulleropyrrolidin-2-yl)-quinolin-8-ol, 2. A solution of C_{60} (190 mg, 0.269 mmol), *N*-methylglycine (48 mg, 0.538 mmol), and 5-formyl-8-hydroxyquinoline (140 mg, 0.808 mmol) in toluene (100 mL) was heated at reflux for 15 h before the solvent was evaporated. The crude product was purified by column chromatography (silica gel, toluene/ethyl acetate 96:4) to give the product (35 mg, 14%). ^{1}H NMR (300 MHz, CDCl$_3$): $\delta = 8.31$ (d, $J = 8.23$ Hz, 1H), 8.17 (t, $J = 8.60$ Hz, 1H), 7.74 (d, $J = 8.05$,

1H), 7.45 (dd, $J = 8.46$ Hz, 1H), 7.15 (d, $J = 7.13$ Hz, 1H), 5.58 (s, 1H), 5.09 (d, $J = 9.15$ Hz, 1H), 4.39 (d, $J = 9.15$ Hz, 1H), 2.81 ppm (s, 3H). ^{13}C NMR (CDCl$_3$:CS$_2$): 40.53 (N-CH3); 66.57 (N-CH2); 83.25 (N-CH) 109.21, 120.01, 124.28, 124.51, 132.85, 137.81, 139.97, 148.88, 158.10 (hydroxyquinoline), 70.58, 73.58, 136.00, 136.75, 137.50, 139.86, 139.75, 139.70, 141.22, 141.28, 141.73, 141.85, 141.92, 141.98, 142.08, 142.10, 142.20, 142.56, 142.60, 143.00, 144.35, 144.49, 144.60, 145.19, 145.25, 145.38, 145.40, 145.44, 145.50, 145.60, 145.63, 145.75, 145.98, 146.01, 146.18, 146.19, 146.20, 146.30, 147.20, 147.28, 150.82, 153.76, 154.85 (fullerene moiety), UV—vis (PhCN): $\lambda_{max} = 330$, 422.5, 701 nm. Mass (APCI mode in CH$_2$Cl$_2$): calcd, 921.0; found, 921.3.

Instrumentation. ^{1}H NMR spectra were obtained from chloroform-d_1 solutions using a Varian 400 MHz NMR spectrometer with tetramethylsilane as internal standard. The UV—vis spectral measurements were carried out with a Shimadzu model 1600 UV—visible spectrophotometer. The fluorescence emission was monitored by using a Varian Eclipse spectrometer. Cyclic voltammograms were recorded on a EG&G PARSTAT electrochemical analyzer with a three-electrode system. A platinum button electrode was used as the working electrode. A platinum wire served as the counterelectrode and an Ag/AgCl was used as the reference electrode. Ferrocene/ferrocenium redox couple was used as an internal standard. All the solutions were purged prior to electrochemical and spectral measurements using argon gas. The mass spectra were recorded on a Varian 1200 L Quadruple MS using APCI mode in dry CH$_2$Cl$_2$. Matrix-assisted laser desorption/ionization time-of-flight mass spectra (MALDI-TOF-MS) were measured on a Kratos Compact MALDI I (Shimadzu) for metal complex in PhCN with dithranol used as a matrix.

The computational calculations were performed by DFT B3LYP/3-21G(*) methods with Gaussian 03 software package[23] on high speed computers. The graphics of frontier orbitals were generated using the *GaussView* software.

Time-Resolved Transient Absorption Measurements. Femtosecond laser flash photolysis was conducted using a Integra-C laser system and an optical detection system provided by Ultrafast Systems (*Helios*). The source for the pump and probe pulses were derived from the fundamental output of Integra-C laser system (780 nm, 2 mJ/pulse, and fwhm = 130 fs) at a repetition rate of 1 kHz. A second harmonic generator introduced in the path of the laser beam provided 410 nm laser pulses for excitation; 95% of the fundamental output of the laser was used to generate the second harmonic, while 5% of the deflected output was used for white light generation. Prior to generating the probe continuum, the laser pulse was fed to a delay line that provided an experimental time window of 3.2 ns with a maximum step resolution of 7 fs. The pump beam was attenuated at 5 μJ/pulse with a spot size of 2 mm diameter at the sample cell where it was merged with the white probe pulse in a close angle (<10°). The probe beam after passing through the 2 mm sample cell was focused on a 200 μm fiber optic cable which was connected to a CCD spectrograph. Typically, 5000 excitation pulses were averaged to obtain the transient spectrum at a set delay time. The kinetic traces at appropriate wavelengths were assembled from the time-resolved spectral data.

Measurements of nanosecond transient absorption spectrum were performed according to the following procedure. A deaerated solution containing a dyad was excited by a Panther OPO pumped by Nd:YAG laser (Continuum, SLII-10, 4—6 ns fwhm) at $\lambda = 430$ nm. The photodynamics were monitored by continuous exposure to a xenon lamp (150 W) as a probe light and a photomultiplier tube (Hamamatsu 2949) as a detector. Transient spectra were recorded using fresh solutions in each laser excitation. The solution was deoxygenated by argon purging for 15 min prior to measurements.

Time-resolved fluorescence spectra were measured by a Photon Technology International GL-3300 with a Photon Technology

(21) Perrin, D. D.; Armarego, W. L. F.; Perrin, D. R. In *Purification of Laboratory Chemicals,* 4th ed.; Pergamon Press: Elmsford, NY, 1996.
(22) Maggini, M.; Scorrano, G.; Prato, M. *J. Am. Chem. Soc.* **1993**, *115*, 9798—9799.
(23) *Gaussian 03*, Frisch, M. J.; et al. Gaussian, Inc., Pittsburgh PA, 2003.

Table 1. Binding Constants, Electrochemical Redox Potentials (E, V vs Fc/Fc$^+$), Free-Energy Changes for Charge Separation and Charge Recombination, and Rate Constants of Forward and Reverse Electron Transfer for the Metal Quinolinolate-Fullerene Complexes in Benzonitrile

compd[a]	log K	M−C Å[b]	MQ$_n$$^{0/+c}$	C$_{60}$$^{0/-}$	ΔG_{CR}[d]	ΔG_{CS}[e]	k_{CS} s^{-1f}	k_{CS} s^{-1g}
1	—	—	1.14	−1.01	−2.15	—	—	6.4 × 10^8
2	—	—	1.21	−1.02	−2.13	—	—	7.7 × 10^8
Al**1**$_3$	10.7	8.5	0.85	−1.01	−1.86	−0.98	3.7 × 10^8	3.9 × 10^8
Al**2**$_3$	9.5	10.3	0.84	−1.02	−1.86	−0.98	3.3 × 10^8	3.2 × 10^8
Zn**1**$_2$	7.2	8.4	1.08	−1.01	−2.09	−0.64	4.1 × 10^8	4.6 × 10^8
Zn**2**$_2$	6.2	10.1	1.06	−1.02	−2.08	−0.65	3.5 × 10^8	3.7 × 10^8

[a] See Chart 1 for structures. [b] Distance between and metal and the center of C$_{60}$. [c] E_{pa} at 100 mV/s. [d] $\Delta G_{CR} = e(E_{ox} - E_{red})$; error = ±10−15%. [e] $-\Delta G_{CS} = \Delta E_{0-0} - \Delta G_{CR}$, where ΔE_{0-0} is the energy of the donor singlet excited state, being 2.73 and 2.84 eV for ZnQ$_2$ and AlQ$_3$ complexes. [f] The k_{CS} was calculated from following equation using fluorescence lifetime data: $k_{CS} = (1/\tau_f)_{sample} - (1/\tau_f)_{ref}$ where $(\tau_f)_{ref}$ is the lifetime of pristine metal−quinolinolate complexes. [g] Calculated from the femtosecond flash photolysis studies by monitoring the decay of the fullerene anion radical band. Error = ±15%.

International GL-302, nitrogen laser/pumped dye laser system, equipped with a four channel digital delay/pulse generator (Stanford Research System Inc. DG535) and a motor driver (Photon Technology International MD-5020). The excitation wavelength was 340 nm using terphenyl (Dojindo Co., Japan) as a dye.

Results and Discussion

Formation of Aluminum and Zinc Complexes of Hydroxyquinoline-Fullerene, 1 and 2. As mentioned earlier, formation of luminescent aluminum−quinolinolate and zinc−quinolinolate complexes with 1:3 and 1:2 molecular stoichiometries is very well-known in the literature.[24] Under the present solution conditions of benzonitrile, the complexation titrations were repeated to ascertain their molecular stoichiometry and binding constants. As shown in the Supporting Information (see Figure S1), such spectral titrations followed by the data analyses yielded the anticipated molecular stoichiometry with high binding constants. The binding constants, log K, were found to be 11.3 and 7.6 for the formation of AlQ$_3$ and ZnQ$_2$ complexes, respectively, in agreement with the literature values (Table 1).[24] Generally, during the titration of hydroxyquinoline with either of the metal ions, the 315 nm absorption band of the ligand revealed diminished intensity with the appearance of a new band around 370 nm corresponding to the metal−quinolinolate complex. One or more isosbestic points were also observed suggesting the existence of an equilibrium process in solution.

In benzonitrile, both **1** and **2** revealed a strong absorption band around 325 and a sharp band at 432 nm. The sharp band was ascribed to the fullerene entity while the 325 nm band was due to the overlap of absorption bands of both 8-hydroxyquinoline and fullerene entities. As shown in Figure 1, addition of Zn^{2+} revealed diminished intensity of the 325 nm band. Owing to the overlap of the high absorbing fullerene and quinoline absorption bands in the spectral region, the observed spectral changes were less than that observed for ZnQ$_2$ formation (see Figure S1). In addition, the 432 nm band corresponding to the fullerene entity exhibited a blue shift of 3 nm indicating substantial interactions between the metal quinolinolate and fullerene entities. The spectral changes at 325 nm were
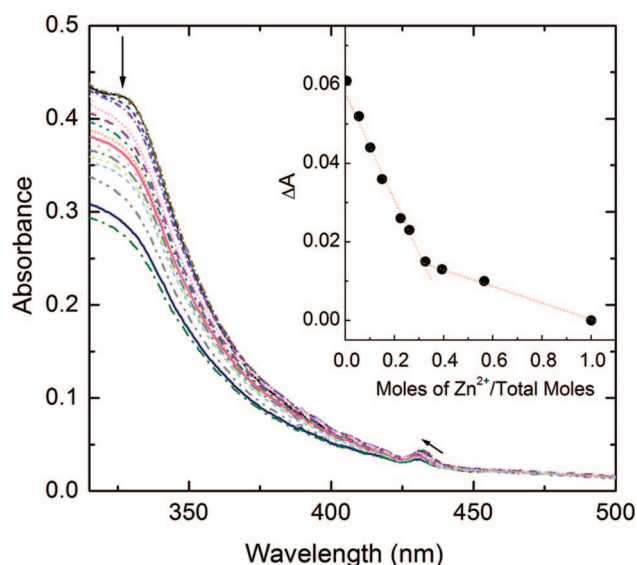

Figure 1. Optical absorption spectrum of **2** (10 µM) on increasing addition of ZnCl$_2$ to form Zn**2**$_2$ in benzonitrile (each addition is 0.1 equiv). The figure inset shows a plot constructed using the mole ratio method to obtain the molecular stoichiometry.

monitored to obtain the molecular stoichiometry using the method of continuous variation and binding constants. A 1:2 stoichiometric mole ratio was obtained indicating the formation of Zn**2**$_2$ complex in solution (Figure 1 inset).

Similar results were also obtained during the titration involving Zn^{2+} and **1** indicating the formation of Zn**1**$_2$. In the case of Al^{3+}, both **1** and **2** binding revealed the expected 1:3 molecular stoichiometry with slightly higher values of binding constants. That is, the formation of Al**1**$_3$ and Al**2**$_3$ was confirmed in benzonitrile solution. The calculated binding constants, log K, were found to be 7.2 and 6.2 for Zn**1**$_2$ and Zn**2**$_2$, and 10.7 and 9.5 for Al**1**$_3$ and Al**2**$_3$ complexes, respectively (Table 1). Although these binding constants are nearly an order of magnitude smaller than that obtained for the formation of AlQ$_3$ and ZnQ$_2$ complexes, stable complex formation is realized from these optical binding data. Further, MALDI-TOF-MS studies were performed to ascertain the metal−ligand complex stoichiometry. As shown in Figure S2 in SI, the Al complexes revealed molecular ion peaks corresponding to the formation of Al**1**$_3$ and Al**2**$_3$ while the Zn complexes revealed molecular ion peaks corresponding to Zn**1**$_2$ and Zn**2**$_2$ thus confirming the complex stoichiometry deduced from optical spectral methods.

Computational Modeling Studies. Our attempts to obtain X-ray quality crystals of these complexes were so far not successful. In the absence of X-ray structures, computational studies were performed at the B3LYP/3-21G(*) level[25,26] to visualize the geometry and electronic structure of the metal oxinate−fullerene(s) donor−acceptor complexes. For this, the fullerene derivatives **1** and **2**, as well as the metal complexes were optimized on a Born−Oppenheimer potential energy surface and a global minima was obtained.

The optimized structures of the starting compounds, fullerene **1** and **2** revealed no steric hindrance between the hydroxyquino-

(24) (a) Steger, H. F.; Corsini, A. *J. Inorg. Nucl. Chem.* **1973**, *35*, 1621–1636. (b) Friedrich, A.; Schilde, U.; Uhlemann, E. *Z. Anorg. Allg. Chem.* **1986**, *534*, 199–205. (c) Matrosovich, T. Y.; Lobanov, F. I.; Makorov, N. V. *Z. Neorg. Khim.* **1986**, *31*, 1441–1446. (d) Enamullah, M.; Ahmed, M. G.; Akhtar, F. *Nucl. Sci. Appl.* **1990**, *2*, 57–71.

(25) For a general review on DFT applications at the B3LYP/3-21G(*) level, see: Zandler, M. E.; D'Souza, F. *C. R. Chemie* **2006**, *9*, 960–981.

(26) For a DFT study with gradient-corrected functionals of metal−quinolinolate complexes see: Curioni, A.; Andreoni, W. *J. Am. Chem. Soc.* **1999**, *121*, 8216–8220.
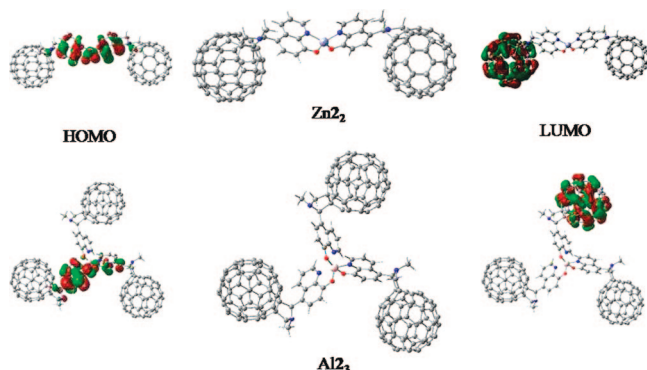
Figure 2. B3LYP/3-21G(*) optimized structures of (a) Zn2₂ and (b) Al2₃. The HOMO and LUMO are shown on the right-hand side and left-hand side of the respective complexes.

line and fullerene entities restraining their access to metal−quinolinolate complex formation (see Figure S3 in SI). Interestingly, the generated HOMO and LUMO orbitals were found to be on the quinoline and fullerene entities, respectively, although part of HOMO was extended to the fulleropyrrolidine carbons. The calculated gas phase HOMO−LUMO gap was found to be 2.45 and 2.38 eV, respectively, for **1** and **2**. These results suggest that both **1** and **2** could act as donor−acceptor dyads, and an excited-state electron transfer in these dyads is a possibility although the HOMO−LUMO gap is relatively larger compared to the values for donor−acceptor dyads reported in the literature.[12−16]

The structures of the zinc quinolinolate−fullerene, Zn2₂, and aluminum quinolinolate−fullerene, Al2₃, donor−acceptor conjugates are shown in Figure 2. The metal complex structures originated from **1** are given in the Supporting Information (see Figure S4). It may be mentioned here that in these calculations three to four different starting geometries for each these complexes were employed and the structures shown here are for the least energy ones for metal−ligand stoichiometric ratio determined by spectroscopic methods, discussed above. The coordination sphere of Zn1₂ and Zn2₂ revealed a tetrahedral geometry which agreed with the earlier studies reported by Nicolau et al. for ZnQ₂ which predicted a distorted tetrahedral or distorted planar depending upon the employed theoretical method.[27] It may be mentioned here that the ZnQ₂ crystals grown from the vapor phase revealed a tetrameric structure (ZnQ₂)₄ with distinct Zn²⁺ ion centers with six- and five-coordination geometry, respectively.[28] Such complex oligomeric structures may not be possible in the case of **1** and **2** binding to Zn²⁺ owing to the presence of bulky fullerene. In the optimized structure, the distance between zinc and center of fullerene was estimated to be ~8.41 Å for Zn1₂ and ~10.1 Å for Zn2₂. The center-to-center distance between the fullerene entities was estimated to be ~15.8 Å for Zn1₂ and ~19.7 Å for Zn2₂, respectively (Table 1). For both complexes, the majority of the HOMO was located on the zinc−quinolinolate segment with appreciable contribution on the fulleropyrolidine carbons, while the LUMO was entirely located on the fullerene entity. The delocalization of HOMO suggests appreciable interaction between the donor and acceptor entities of the dyad, a result that readily agrees with the optical absorption spectral results. The gas phase HOMO−LUMO gap was found to be ~1.85 and

~1.88 eV, respectively, for Zn1₂ and Zn2₂, significantly smaller than that calculated for either **1** or **2**.

The coordination sphere of Al1₃ and Al2₃ revealed an octahedral geometry around the Al center, similar to that reported by experimental[6,29] and computational[26,30] studies of aluminum−quinolinolate complexes. The average distance between aluminum and center of fullerene was estimated to be ~8.5 Å for Al1₃ and ~10.3 Å for Al2₃, respectively. The center-to-center distance between the fullerene entities was estimated to be ~14.1 Å for Al1₃ and ~17.7 Å for Al2₃, respectively. The three fullerene entities were positioned roughly in an equilateral triangle. Similar to the zinc complexes, the majority of the HOMO was located on the aluminum−quinolinolate segment with appreciable amount on the fulleropyrrolidine carbons while the LUMO was entirely located on the fullerene entity. This again suggests appreciable interactions between the donor and acceptor entities of the dyad. The gas phase HOMO−LUMO gap was found to be ~1.79 and ~1.71 eV for Al1₃ and Al2₃, respectively, significantly smaller than that calculated for either **1** or **2**. These results suggest formation of a new series of donor−acceptor conjugates in which the metal−quinolinolate segment acts as an electron donor and fullerene acts as an electron acceptor, and considerable electronic interactions occur between these entities. Such studies also show variation of donor−acceptor distances to some extent by the choice of substitution at either the 2- or 5-positions of hydroxyquinoline.

Electrochemical Redox Behavior and Energy Levels. Electrochemical studies using cyclic voltammetric technique were performed to evaluate the redox potentials of **1** and **2** and the resulting Zn and Al complexes. Figure 3 shows representative cyclic voltammograms of **1** and its respective in situ generated Zn and Al complexes. The first two one-electron reductions of **1** were located at $E_{1/2} = -1.01$ and -1.42 V vs Fc/Fc⁺ in benzonitrile, 0.1 M (TBA)ClO₄. On the anodic side, an irreversible oxidation at $E_{pa} = \sim 1.14$ V vs Fc/Fc⁺ corresponding to the oxidation of hydroxyquinoline entity was observed. Similar voltammetric behavior was also observed for compound **2**.

Addition of stoichiometric amounts of either Zn²⁺ or Al³⁺ to form the respective Zn1₂ and Al1₃ complexes revealed cathodic shifts up to 150 mV for the oxidation waves (see Figure 3 solid lines). The peaks corresponding to the fullerene reductions revealed no significant changes; however, scanning the potential beyond the second reduction caused appreciable decrease in the anodic peak current, suggesting considerable decomposition of the second one-electron reduced product of these complexes.

In a control experiment, the cyclic voltammograms of HQ, ZnQ₂, and AlQ₃ were also recorded (see Figure S5 in SI). The redox chemistry of the HQ and the resulting complexes were found to be quasi-reversible to irreversible processes.[2g,h] An irreversible reduction process was observed at $E_{pc} = -2.4$ V vs Fc/Fc⁺ (at a scan rate of 100 mV/s) for all of these compounds. Owing to the similarity of the redox potential and

(27) Nicolau, D. V.; Yoshikawa, S. *J. Mol. Graphics Model* **1998**, *16*, 83.
(28) Kai, Y.; Moraita, M.; Yasuka, N.; Kasai, N. *Bull. Chem. Soc. Jpn.* **1985**, *58*, 1631–1635.

(29) (a) Cölle, M.; Dinnebier, R. E.; Brötting, W. *Chem. Commun.* **2002**, 2908–2909. (b) Brinkmann, M.; Gadret, G.; Muccini, M.; Taliani, C.; Masciocchi, N.; Sironi, A. *J. Am. Chem. Soc.* **2000**, *122*, 5147–5157. (c) Braun, M.; Gmeiner, J.; Tzolov, M.; Cölle, M.; Meyer, F.; Milius, W.; Hillebrecht, H.; Wendland, O.; von Schutz, J.; Brütting, W. *J. Chem. Phys.* **2001**, *114*, 9625.
(30) (a) Curioni, A.; Boreo, M.; Andreoni, W. *Chem. Phys. Lett.* **1998**, *294*, 263. (b) Curioni, A.; Andreoni, W.; Treusch, R.; Himpsel, F. J.; Haskal, E.; Seidler, P.; Heske, C.; Kakar, S.; van Buuren, T.; Terminello, L. J. *Appl. Phys. Lett.* **1998**, *72*, 1575.
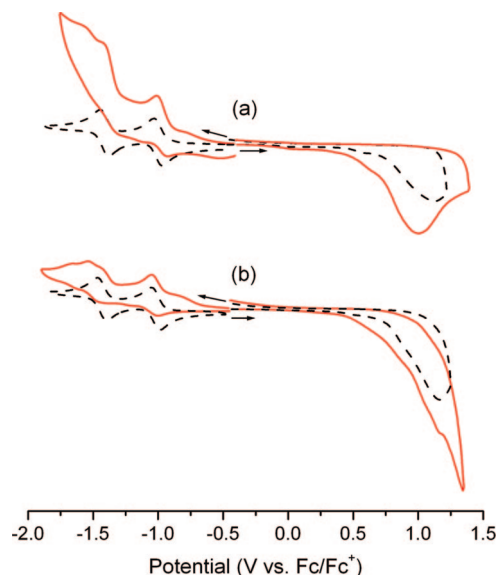
Figure 3. Cyclic voltammograms showing the oxidation and reduction of **1** in the absence of added metal ions (dotted lines in a and b) and in the presence of Zn^{2+} to form $Zn\mathbf{1}_2$ complex (solid line in a) and Al^{3+} to from $Al\mathbf{1}_3$ (solid line in b) in benzonitrile, 0.1 M (TBA)ClO_4. Scan rate = 100 mV/s.
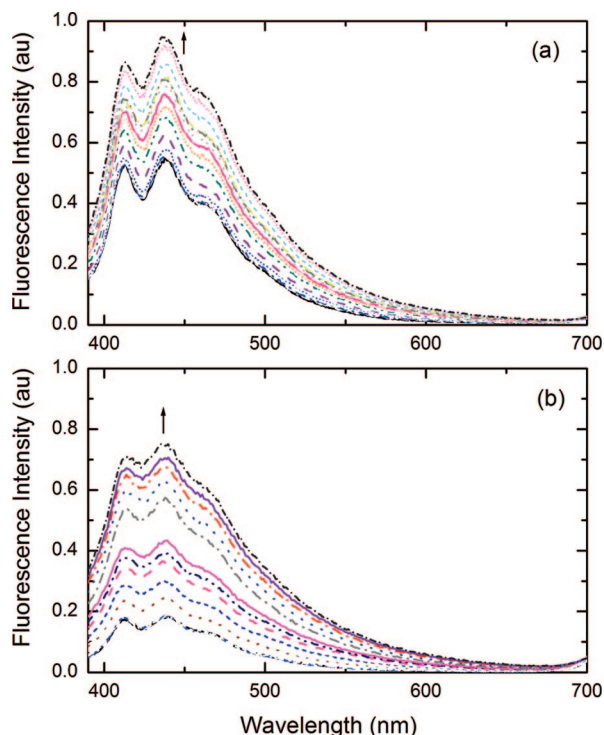

Figure 4. Steady-state fluorescence spectra of **2** (50 μM) showing signal enhancement during the formation of (a) $Zn\mathbf{2}_2$ and (b) $Al\mathbf{2}_3$ complexes in benzonitrile, λ_{ex} = 365 nm.

waves, these processes were attributed to the reduction of the HQ entity. The E_{pa} corresponding to the first oxidation of HQ, ZnQ_2, and AlQ_3 were located at 0.76, 0.66, and 0.72 V vs Fc/Fc$^+$, respectively. That is, the metal complexes were easier to oxidize compared to the HQ,[2g,h] an observation that readily followed to that of the metal complexes of **1** and **2**, discussed above.

The energy levels of the charge-separation and charge-recombination states were estimated using the Weller-type
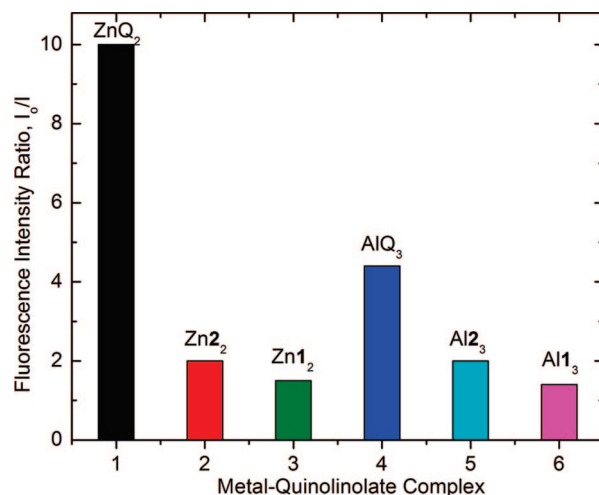

Figure 5. Bar chart showing fluorescence intensity enhancement for the Zn and Al complexes of HQ, **1**, and **2** in benzonitrile. I_0 and I indicate emission intensity of free and metal bound HQ, **1**, and **2**.
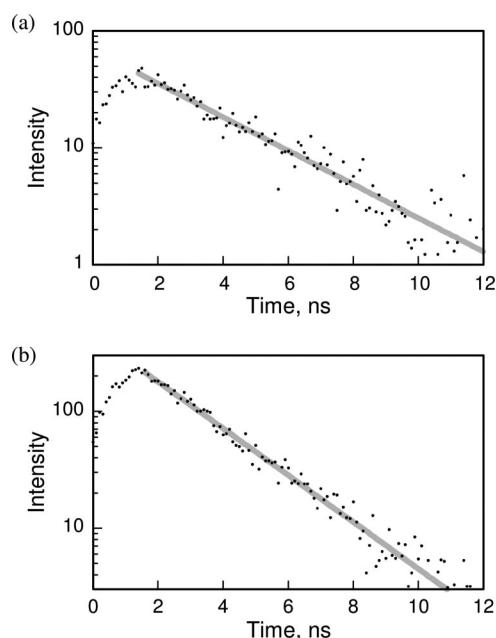

Figure 6. Representative fluorescence decay profiles of (a) $Zn\mathbf{1}_2$ and (b) $Al\mathbf{1}_3$ in benzonitrile. The samples were excited at 340 nm and the emission was collected at 400 nm. The complexes were generated in situ by mixing stoichiometric amounts of metal halide and ligand in benzonitrile.

approach[31] utilizing the redox potentials and the energy levels of the singlet excited states, as listed in Table 1. The generation of $MQ_n^{\cdot+}-C_{60}^{\cdot-}$ is exothermic via the singlet excited states of the metal−quinolinolates in benzonitrile, more so for the Al complexes. It may be mentioned here that owing to the irreversible oxidation of MQ_n, an error of 10−15% may be assumed in the calculated energy states.

(31) (a) Rehm, D.; Weller, A. *Isr. J. Chem.* **1970**, *7*, 259. (b) Mataga, N.; Miyasaka, H. In *Electron Transfer*; Jortner, J., Bixon, M., Eds.; John Wiley & Sons: New York, 1999; Part 2, pp 431−496.

(32) (a) Ballard, R. E.; Edwards, J. W. *J. Chem. Soc.* **1964**, 4868−4874. (b) Goldman, M.; Wehry, E. L. *Anal. Chem.* **1970**, *42*, 1178−1185. (c) Bronson, R. T.; Montalti, M.; Prodi, L.; Zaccheroni, N.; Lamb, R. D.; Dalley, N. K.; Izatt, R. M.; Bradshaw, J. S.; Savage, P. B. *Tetrahedron* **2004**, *60*, 11139−11144. (d) Farruggia, G.; Iotti, S.; Prodi, L.; Montalti, M.; Zaccheroni, N.; Savage, P. B.; Trapani, V.; Sale, P.; Wolf, F. I. *J. Am. Chem. Soc.* **2006**, *128*, 344−350.
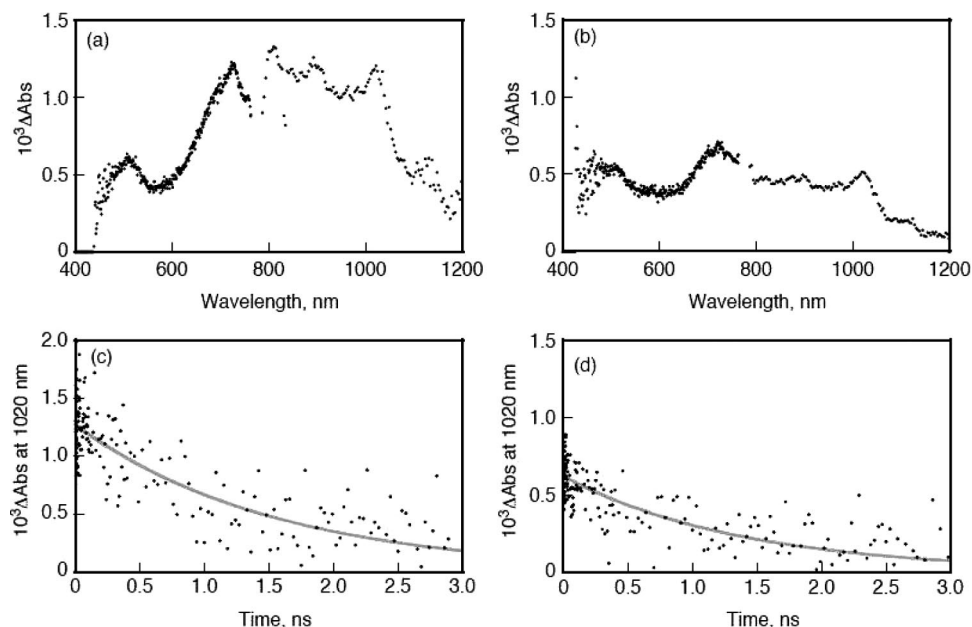
Figure 7. Transient absorption spectrum of (a) **1** and (b) **2** in benzonitrile taken at 200 ps. The lower panels show the decay of the 1020 nm corresponding to $C_{60}^{•−}$.
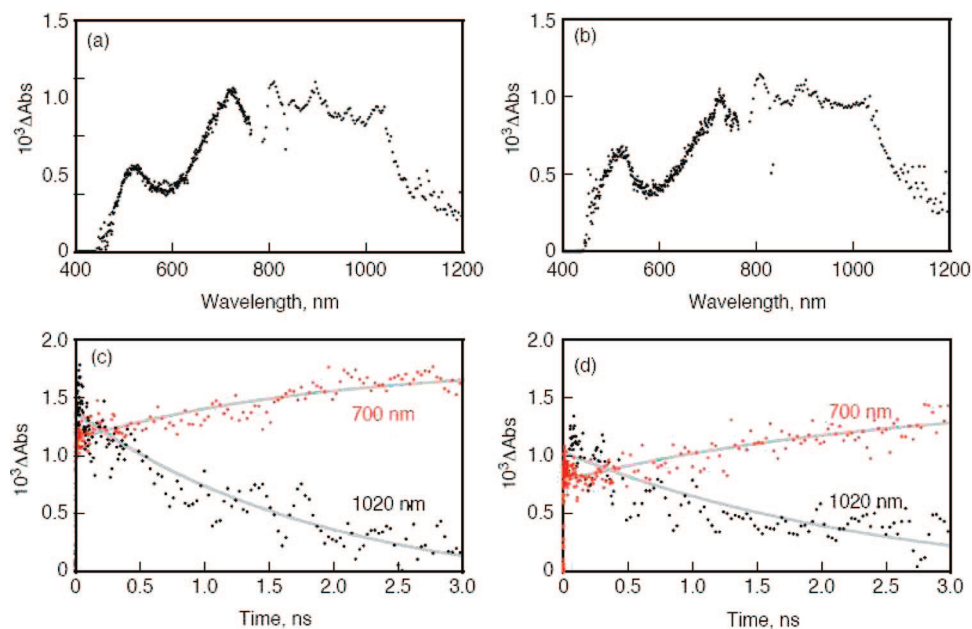

Figure 8. Transient absorption spectrum of (a) $Zn\mathbf{1}_2$ and (b) $Al\mathbf{1}_3$ in benzonitrile taken at 200 ps. The lower panels shows the rise of the 700 nm peak corresponding to fullerene triplet state and decay of the 1020 nm corresponding to fullerene anion radical, $C_{60}^{−•}$. The complexes were in situ formed by stoichiometric additions of the metal and the ligand.

Steady-State Fluorescence Studies. In agreement with the literature results,[32] the fluorescence spectrum of HQ in benzonitrile revealed bands in the 400−480 nm region. Addition of metal ions to the solution immediately resulted in the generation of a new strong emission band at 552 nm for Zn^{2+} addition and 510 nm for Al^{3+} addition indicating formation of higher fluorescent metal quinolinolate complexes (see Figure S6 in Supporting Information).[33] The emission behavior of **1** and **2**, having two fluorophores, namely, 8-hydroxyquinoline and fullerene, was found to be similar to that of HQ with bands in the 400−480 nm region, in addition to a weak emission band around 720 nm corresponding to the fullerene entity. Addition of either Zn^{2+} or Al^{3+} to the solution immediately resulted in fluorescence enhancement; however, the band position was blue-shifted, causing it to overlap with the emission spectrum of the starting compounds, **1** and **2** (Figure 4 and Supporting Information, Figure S7).

It is important to note that upon formation of the $MQ_n−C_{60}$ complexes, the band at 720 nm corresponding to fulleropyrrolidine emission did not show any appreciable changes in the intensity or position (Supporting Information, Figure S8). These results suggest the absence of excited-state energy transfer from excited metal quinolinolate complex to the fullerene entity.

(33) (a) Ballardini, R.; Varani, G.; Indelli, M. T.; Scandola, F. *Inorg. Chem.* **1986**, *25*, 3858−3865. (b) Rollier, H.; Ryan, D. E. *Anal. Chim. Acta* **1975**, *74*, 23−28. (c) Lytle, F. E.; Storey, D. R.; Juricich, M. E. *Spectrochem. Acta, A* **1973**, *29*, 1357−1369. (d) Ohnesorge, W. E.; Rogers, L. B. *Spectrochem. Acta* **1959**, 27−40.
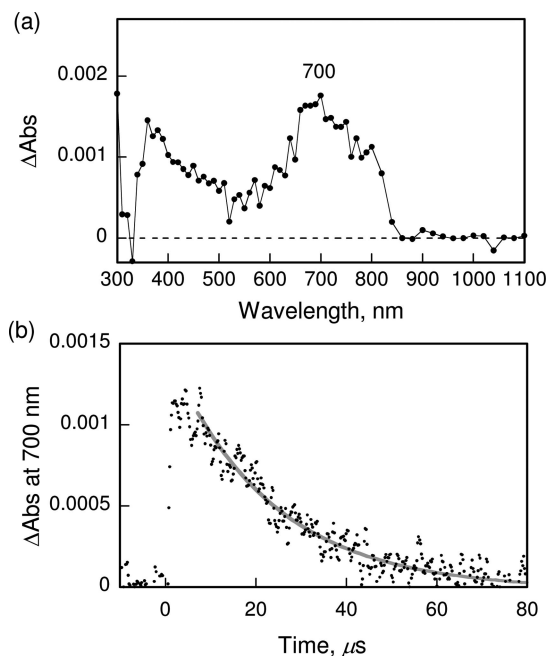
Figure 9. (a) Transient absorption spectrum of Al1_3 in benzonitrile taken at 10 μs. (b) Time profile of the decay of absorbance at 700 nm due to the triplet excited-state of C$_{60}$.
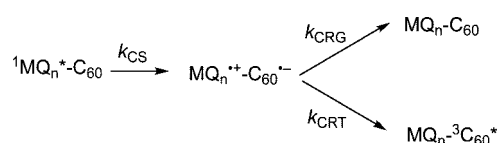
Scheme 1

Figure 5 shows a bar chart of fluorescence intensity ratio enhancement for HQ, **1**, and **2** after the formation of respective metal complexes. Analyses of such a plot revealed the following: (i) The Zn complexes exhibit higher level of metal binding-induced fluorescence enhancement compared to their Al analogues. (ii) The fluorescence enhancement follows the order: M1_n < M2_n < MQ$_n$ (M = Al and n = 3; M = Zn and n = 2), that is, when the fullerene is in M2_n and M1_n complexes, substantial quenching of the fluorescence is observed. For reasons discussed earlier, excited-state energy transfer as one of the quenching mechanisms can be ruled out. Time-resolved emission and transient absorption spectral studies were systematically performed to unravel the quenching mechanism in these newly formed donor−acceptor complexes.

Time-Resolved Emission and Transient Absorption Studies. Time resolved studies on the picosecond time scale were performed to establish the occurrence of electron transfer and to evaluate their kinetics. The time-resolved emission spectrum of ZnQ$_2$ and AlQ$_3$ in benzonitrile revealed mono-exponential decay from which the fluorescence lifetime were evaluated to be 21 and 19 ns (see Supporting Information, Figure S9 for decay curves), respectively, in agreement with the values reported in the literature.[33] Interestingly, the lifetime of **1** and **2** in deaerated benzonitrile, with an excited wavelength of 340 and emission monitoring wavelength of 400 nm, were found to be quenched significantly. The evaluated lifetimes were found to be 3.02 and 2.17 ns, respectively, for **1** and **2** suggesting occurrence of excited-state events.

Figure 6 shows representative fluorescence decay curves for Zn1_2 and Al1_3, respectively. All of the decay curves could be

fitted to a monoexponential decay implying existence of ∼100% metal ion-bound donor−acceptor complexes of **1** and **2**.

Substantial quenching of the metal−quinolinolate lifetime for all of the donor−acceptor complexes was observed, suggesting the occurrence of photochemical events from the singlet excited MQ$_n$ segment to the fullerene entity. By assuming the quenching is due to excited-state electron transfer, the rates of charge separation, k_{CS}, were calculated for the zinc and aluminum complexes (Table 1). The magnitudes of k_{CS} suggest a fairly efficient process, and such events are slightly more efficient for complexes generated from **1** compared to those generated from **2**. This could be rationalized in terms of the close proximity of the donor−acceptor entities in the case of Zn1_2 and Al1_3 complexes, discussed earlier. In addition, intraligand charge transfer between the phenolato- and pyridinato- moieties may also play some role in governing the magnitude of k_{CS}.

Further femtosecond transient absorption studies were performed to identify the electron transfer products and to track their fate. Figure 7 shows time-resolved transient absorption spectra of **1** and **2** observed by femtosecond laser flash photolysis in deaerated benzonitrile. As predicted, both of the hydroxyquinoline appended fullerene derivatives prior to the formation of metal complexes revealed transient spectral features suggesting occurrence of electron transfer from excited hydroxyquinoline to the fullerene entity. That is, an absorption band at 1020 nm was observed in each case corresponding to the formation of a fulleropyrrolidine radical anion. An additional broadband around 700 nm was also observed corresponding to the triplet excited states of fullerene.[34,35]

Figure 8 shows the transient absorption spectrum of the Zn1_2 and Al1_3 complexes in benzonitrile while the corresponding spectrum of the Zn2_2 and Al2_3 complexes are given in the Supporting Information (see Figure S9). All of these metal complexes revealed transient spectral signature of fullerene anion radical at 1020 nm. Additional bands in the visible region were also observed corresponding to the triplet state of the fullerene.

As shown by the time profiles of the peaks in Figure 8 and Supporting Information, Figure S10, the decay of absorbance at 1020 nm due to the CS state was accompanied by the rise in absorbance at 700 nm due to the triplet excited-state of C$_{60}$ (^{3}C$_{60}$*) indicating occurrence of back electron transfer populating the triplet excited state. However, the yield of ^{3}C$_{60}$* determined by the nanosecond laser flash photolysis measurements (Figure 9) was found to be 0.02. Such a small yield of the triplet excited-state suggests that there is an alternative and faster decay pathway from the CS state that should be the back electron transfer to the ground state. In such a case, the apparent decay rate of the CS state corresponds to the rate of formation of the CS state as shown in Scheme 1 (see the pertinent equations discussed below). The lifetime of the ^{3}C$_{60}$* from the decay plot in Figure 9b was found to be 23 μs, close to that reported in the literature for functionalized fullerenes.[35]

(34) (a) Guldi, D. M; Maggini, M.; Scorrano, G.; Prato, M. *J. Am. Chem. Soc.* **1997**, *119*, 974–980. (b) D'Souza, F.; Zandler, M. E.; Smith, P. M.; Deviprasad, G. R.; Arkady, K.; Fujitsuka, M.; Ito, O. *J. Phys. Chem. A* **2002**, *106*, 649–656.

(35) (a) Imahori, H.; Tamaki, K.; Guldi, D. M.; Luo, C.; Fujitsuka, M.; Ito, O.; Sakata, Y.; Fukuzumi, S. *J. Am. Chem. Soc.* **2001**, *123*, 2607–2617. (b) Imahori, H.; Guldi, D. M.; Tamaki, K.; Yoshida, Y.; Luo, C.; Sakata, Y.; Fukuzumi, S. *J. Am. Chem. Soc.* **2001**, *123*, 6617–6628. (c) Fukuzumi, S.; Ohkubo, K.; Imahori, H.; Shao, J.; Ou, Z.; Zheng, G.; Chen, Y.; Pandey, R. K.; Fujitsuka, M.; Ito, O.; Kadish, K. M. *J. Am. Chem. Soc.* **2001**, *123*, 10676–10683.

The pertinent differential equations and their solutions for the formation and decay of the CS state employed to analyze the data presented in Figures 8 and S9 are described:

$$-d[^1D* - C_{60}]/dt = k_{CS}[^1D* - C_{60}] \quad (1)$$

$$[^1D* - C_{60}] = [^1D* - C_{60}]_0 \exp(-k_{CS}t) \quad (2)$$

$$d[D^{\bullet+} - C_{60}^{\bullet-}]/dt = k_{CS}[^1D* - C_{60}] - (k_{CRG} + k_{CRT})[^1D* - C_{60}] \quad (3)$$

Equation 2 is substituted into eq 3. Then each term is multiplied by $\exp[-(k_{CRG} + k_{CRT})t]$ to afford

$$\exp[(k_{CRG} + k_{CRT})t] \, d[D^{\bullet+} - C_{60}^{\bullet-}]/dt = \exp[(k_{CRG} + k_{CRT})t][D^{\bullet+} - C_{60}^{\bullet-}](k_{CRG} + k_{CRT}) = k_{CS}[^1D* - C_{60}]_0 \exp[(k_{CRG} + k_{CRT} - k_{CS})t] \quad (4)$$

By integrating eq 4 with $[D^{\bullet+} - C_{60}^{\bullet-}] = 0$ at $t = 0$, eq 5 is derived.[36]

$$[D^{\bullet+} - C_{60}^{\bullet-}] = k_{CS}[^1D* - C_{60}]_0[\exp(k_{CS}t) - \exp\{-(k_{CRG} + k_{CRT} - k_{CS})t\}]/(k_{CRG} + k_{CRT} - k_{CS}) \quad (5)$$

Under the conditions such that $k_{CRG} + k_{CRT} \gg k_{CS}$, eq 5 is simplified as given by eq 6, which indicates that the single exponential decay of $[D^{\bullet+} - C_{60}^{\bullet-}]$ affords the CS rate constant (k_{CS}).

$$[D^{\bullet+} - C_{60}^{\bullet-}] = k_{CS}[^1D* - C_{60}]_0[\exp(k_{CS}t)]/(k_{CRG} + k_{CRT}) \quad (6)$$

The k_{CS} values determined from the decay of absorbance at 1020 nm due to the CS state agree well within experimental errors with those determined from the fluorescence decay (Table 1). Such agreement between the fluorescence decay rate and the CS decay rate is required to confirm that the CS rate is much slower than the CR rate,[37] as discussed in the preceding paragraphs.

Conclusions

The present study successfully demonstrates the electron donor characteristics of metal quinolinolate complexes used in organic LED when suitably connected to a well-known electron acceptor like fullerene. The 8-hydroxyquinoline functionalized fullerene for this purpose formed stable, fluorescent complexes with zinc(II) and aluminum(III) metal ions. Computational, electrochemical, and optical absorption and emission studies demonstrated the electron donor—acceptor nature of the metal quinolinolate—fullerene complexes and the free energy calculations suggested the possibility of the occurrence of photoinduced electron transfer from singlet excited metal quinolinolate to the fullerene entity. The charge-separation processes via $^1MQ_n*$ (for M = Al and n = 3, and M = Zn and n = 2) moiety were initially monitored by time-resolved fluorescence quenching methods. Generally, by increasing the donor—acceptor distance, a decrease in k_{CS} was observed for the investigated donor—acceptor complexes. Femtosecond time-resolved transient absorption studies confirmed occurrence of photoinduced electron transfer in which one of the electron transfer products, fullerene anion radical in the near-IR region was easily detected. Detailed analysis of the kinetic data in this novel series donor—acceptor conjugates revealed occurrence of faster charge recombination compared to charge separation, and decay of the charge separated state to populate the low-lying fullerene triplet state in competition with direct charge recombination to the ground state.

Supporting Information Available: Complete ref 23; absorption and emission spectral changes during the formation of AlQ_3 and ZnQ_2, MALDI-TOF-MS spectra of the metal quinolinolate—fullerene complexes, optimized structures, HOMO and LUMO of **1**, **2**, Zn**1**$_2$, and Al**1**$_3$, cyclic voltammograms of HQ, AlQ_3, and ZnQ_2, fluorescence emission during the formation of Zn**1**$_2$ and Zn**2**$_2$, fluorescence decay profiles of ZnQ_2 and AlQ_3, and femtosecond transient absorption spectrum of Zn**2**$_2$ and Al**2**$_3$ in benzonitrile. This material is available free of charge via the Internet at http://pubs.acs.org.

JA805027R

(36) For the general kinetic analysis for consecutive reactions, see: Espenson, J. H. *Chemical Kinetics and Reaction Mechanisms*; McGraw-Hill: New York, 1981; 65—69.

(37) Imahori, H.; Yamada, H.; Guldi, D. M.; Endo, Y.; Shimomura, A.; Kundu, S.; Yamada, K.; Okada, T.; Sakata, Y.; Fukuzumi, S. *Angew. Chem., Int. Ed.* **2002**, *41*, 2344–2347.